

# Prediction of Engine Noise using Parameterized Combustion Pressure Curves

José Scarpati, Adam Wikström, Ola Jönsson, Ragnar Glav  
SCANIA CV, Södertälje, Sweden

Peter Händel, Håkan Hjalmarsson

School of Electrical Engineering, Royal Institute of Technology, Stockholm, Sweden

Copyright © 2007 SAE International

## ABSTRACT

A parameterization for combustion chamber cylinder pressures is tuned to measurements on an inline 6 cylinder Diesel engine at different operating conditions. Both measured and modeled signals are filtered in the frequency domain and according to the so called Lucas attenuation. Two different estimates of engine radiated noise are obtained and compared in this fashion. The influence of physically meaningful parameters on the frequency contents of the final noise level is analyzed, as well as the contribution of the pressure trace of the motored engine. The scattering of data in the pressure signal is calculated as a function of the crank angle allowing for statistical considerations.

## INTRODUCTION

Contemporary engine development on commercial vehicles is pushed by both stricter legal limitations on exhaust emissions as well as customer demands on improved fuel economy. Different solutions combining exhaust after treatment and alternative combustion strategies, typically with increased energy release rates, are topics of current research. The latter results in higher engine noise and is thus in conflict with the tightened legal requirements concerning environmental noise. Obviously, engine noise prediction in the early stages of development has gained crucial importance.

The combustion process is one of the main sources of engine noise and is even predominant, over the mechanical contribution at lower values of RPM and load. In the present work, the combustion chamber pressure is measured in an inline 6-cyl diesel engine at different operating conditions and combustion strategies. A parameterized model of the internal pressure is proposed and the so called *Lucas Filter* is used to predict radiated engine noise for directly measured as well as parameterized pressure, see [3].

The ultimate aim is to produce low-complexity input-output models with physically meaningful parameters that, with reasonable accuracy, are able to predict the frequency content of the radiated combustion noise in the frequency range between 500 Hz and 5 kHz. Since no noise measurements were available in this work the possibility of carrying out a formal validation of the model was limited; hence the focus is placed on the capability of the parameterized-model of reproducing the frequency contents of the original signal and one the parameters representing physical properties.

The model of the cylinder pressure presented here is based on the ideal thermodynamic relationships for polytropic compression and expansion processes; the combustion is modeled with an empirical correlation, exhaust is approximated with an exponential function and intake assumed isobaric.

Results presented in, for instance [1] show high correlation between combustion noise and heat release rate peaks, which points out the critical importance of the combustion model. Nonlinear minimization is used to fit the parameterized pressure trace to crank angle domain measurements. The basic model yields good approximation only at lower frequencies; hence an additional term is added in order to improve the fit for higher frequency ranges. The results include calculated standard deviations in terms of noise levels.

Plans for future work include recording of radiated engine noise synchronized with cylinder pressure and crank shaft speed measurements at different operating conditions. This data will be processed so as to separate combustion and mechanical noise in order to allow for a thorough assessment, upgrading and validation of the approach presented here; including a more complete evaluation of the fit between physical parameters and noise.

## MEASUREMENTS

High precision quartz pressure sensors are mounted into the combustion chamber of a common rail equipped, turbocharged, inline, 6-cylinders, diesel engine. The pressure trace is measured in 50 cycles for different steady state conditions. The range of speeds is selected from 800 RPM to 2300 RPM. Three loads cases are tested: full load (70%), partial load (30%) and motored (zero load). Injection timing is varied according to a standard map where no pilot injection is used.

Figure 1 shows pressure traces in full load and motoring at 800 RPM. The difference in levels outside the combustion interval is mainly due to turbo charging. A steep pressure rise can be seen in this case. The opening of the exhaust valves is clearly identified as well.

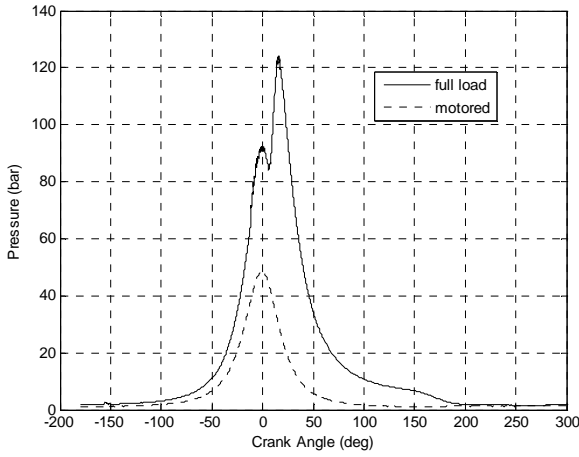


Figure 1. Full load and motored pressure traces at 800 RPM.

## MODEL OF CYLINDER PRESSURE

The model is based on the work presented in [2] where a parameterization based on polytropic expressions and a combustion empirical correlation is applied to a spark ignited or common gasoline engine. Here, a similar approach is taken for a compression ignition or diesel engine. The parameterization is a function of crank angle degrees (CADs), in which 0° corresponds to piston top dead center. Angular magnitudes are given in degrees.

In the current model, the compression and expansion strokes are described as polytropic processes; the exponents are considered as parameters that will be fitted to measurements. The Vibe function is used as in [2] to approximate the pressure ratio ( $PR$ ) during combustion; introducing in this way the influence of the heat release rate. The pressure ratio reads:

$$PR(\theta) = 1 - e^{-a \left( \frac{\theta - \theta_{soc}}{\Delta\theta} \right)^x}$$

The parameters  $a$ ,  $\Delta\theta$ , and  $x$  will be fitted against a measured pressure trace. In this way the need to compute properties such as the temperature rise under combustion is avoided. The subscript  $soc$  stands for start of combustion, and accordingly  $\theta_{soc}$  is the angle of start of combustion.

The gas exchange phase ( $EX$ ) is included by interpolating between the expansion asymptote and the exhaust manifold pressure with an exponential function, as follows:

$$EX(\theta) = e^{-b \left( \frac{\theta - \theta_{evo}}{10} \right)^y}$$

where the subscript  $\theta_{evo}$  stands for the angular coordinate at opening of the exhaust valves, and where  $b$  and  $y$  are fitting parameters.

The final expression for the pressure as function of  $CAD$  reads:

$$p(\theta) = \begin{cases} p_0, & \theta \leq ivc \\ p_{soc} \left( \frac{V_{soc}}{V(\theta)} \right)^{k_c}, & ivc < \theta \leq soc \\ PR(\theta) p_e(\theta) + (1 - PR(\theta)) p_c(\theta), & soc < \theta \leq eoc \\ p_{eoc} \left( \frac{V(\theta_{eoc})}{V(\theta)} \right)^{k_e}, & eoc < \theta \leq evo \\ p_{ex-ref} (1 - EX(\theta)) + p_{evo} EX(\theta), & \theta > evo \end{cases}$$

Where  $ivc$  denotes intake valves closed and  $eoc$  the end of combustion. Since first derivative requirements are not imposed on the transitions the above parameterization will not necessarily become a smooth function of  $\theta$ .

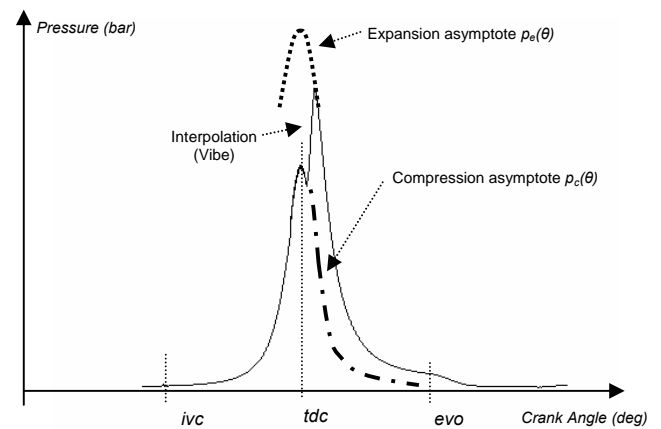


Figure 2 Schematic view of the model

No special modeling considerations are included for the intake valves opening; furthermore the pressure is assumed constant during the intake stroke and its value dependent on the fitting parameter  $p_{soc}$  which is the pressure at the start of combustion. The parameter  $p_{ex-ref}$  is defined as a sort of exhaust reference pressure, since the actual exhaust pressure will turn out higher. Note that the focus is put on the compression, combustion and expansion processes. Figure 2 shows a sketch of the components in the considered model.

## CURVE FITTING PROCEDURE

The presented model contains essentially 12 parameters to be tuned, for notational simplicity hereafter denoted by  $\alpha_1, \dots, \alpha_{12}$ . These can be determined by fitting the model to pressure traces, i.e. by minimizing the sum of squares of the errors

$$\Delta p^2 = \sum_1^m (p_i - f(\theta_i, \alpha_1 \dots \alpha_{12}))^2$$

where  $p_i$  denotes the given pressure at crank angle  $\theta_i$ , and  $m$  the number of sampled pressure values. The numerical problem becomes a non linear least squares fitting which may for instance be solved as presented in [8]. The procedure is broadly outlined below:

Pick an initial guess  $\alpha_j^*$  for the parameters  $\alpha_j$  and define:

$$dp_i = p_i - f(\theta_i, \alpha_j^*)$$

Now obtain a linearized estimate of the changes  $d\alpha_j$  needed to reduce  $dp_i$  to zero,

$$dp_i = \sum_1^n \frac{\partial f}{\partial \alpha_j} d\alpha_j \Big|_{\theta_i, \alpha^*}$$

where  $n$  denotes the number of parameters. This can be written in component form as:

$$dp_i = A_{ij} d\alpha_j$$

where  $d\alpha_j$  becomes an offset in the parameters and  $A$  is the  $m \times n$  matrix

$$A_{ij} = \begin{bmatrix} \frac{\partial f}{\partial \alpha_1} \Big|_{\theta_1, \alpha^*} & \dots & \frac{\partial f}{\partial \alpha_n} \Big|_{\theta_1, \alpha^*} \\ \frac{\partial f}{\partial \alpha_1} \Big|_{\theta_2, \alpha^*} & \dots & \frac{\partial f}{\partial \alpha_n} \Big|_{\theta_2, \alpha^*} \\ \vdots & \ddots & \vdots \\ \frac{\partial f}{\partial \alpha_1} \Big|_{\theta_m, \alpha^*} & \dots & \frac{\partial f}{\partial \alpha_n} \Big|_{\theta_m, \alpha^*} \end{bmatrix}$$

In more concise matrix form we may write:

$$d\vec{p} = A d\vec{\alpha}$$

where  $d\vec{p}$  is a  $m$ -vector and given,  $A$  is the Jacobian matrix also given and  $d\vec{\alpha}$  is a  $n$ -vector; the unknowns. The latter expression constitutes an over determined set of linear equations which may be solved in the least squares sense and in terms the offset vector as:

$$d\vec{\alpha} = (A^T A)^{-1} A^T d\vec{p}$$

This offset is then applied to vector  $\vec{\alpha}$  and the procedure repeated iteratively until the offset becomes smaller than a prescribed tolerance.

In the present work the Matlab function *lsqcurvefit*, which enhances this technique, is chosen to perform the minimization.

As mentioned previously the intention for the model here is to reproduce the frequency content of the original signal. To further improve the performance of the least squares minimization a weighing procedure is applied. As presented in [9], when the different observations are given different weights it is possible to write the minimizing element as:

$$d\vec{\alpha} = (A^T Q_N A)^{-1} A^T Q_N d\vec{p}$$

where  $Q_N$  is a diagonal matrix filled with the weights  $q_i$ , on its diagonal and its effect is filtering of the original observations. The extreme case would be to simply disregard some observation intervals, i.e. give them a zero weight. This weighing scheme is the approach selected here; a conclusion reached after a few trials with filters of different frequency bands. The fitting interval is selected for  $\theta > -10$  CAD, namely a few degrees before start of combustion.

The reference measured curved is obtained by averaging the 50 available cycles for every operating condition. A uniform probability distribution in  $\theta$  is assumed, i.e. every cycle is equally weighed.

## RESULTING PARAMETERS

Tables A2 and A3 report the resulting parameters obtained after tuning, together with two fit indexes, as defined in the appendix, for both the whole trace and the combustion region, the latter between  $-10^\circ$  and  $30^\circ$  CAD. Figures A15 and A16 in the appendix include plots of a few parameters versus RPM in order to facilitate comparison.

The fit indexes exhibit higher values in the combustion range which was to be expected since higher numerical weight was put in modeling this interval. The results obtained for the partial load case show shorter

combustion intervals, as well as lower pressures at both the start and end of combustion.

Parameters such as polytropic exponents, duration of combustion, pressures and even opening of the exhaust valves, all correspond to physically reasonable values. The proximity of the polytropic exponents suggests that perhaps only one parameter could be used instead of two, for this magnitude. On the other hand, parameters like those included in the Vibe correlation are not directly identifiable in measurements making difficult a more complete validation

The use of different combustion strategies, i.e. injection timing and amounts of fuel, impedes drawing precise conclusions on the fluctuations with load and angular speed of the resulting parameters.

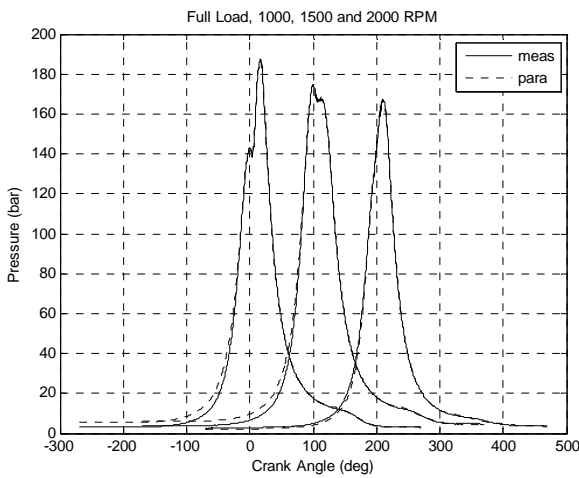


Figure 3. Measured and estimated full load pressure traces. From left to right 1000 RPM, 1500 RPM and 2000 RPM respectively.

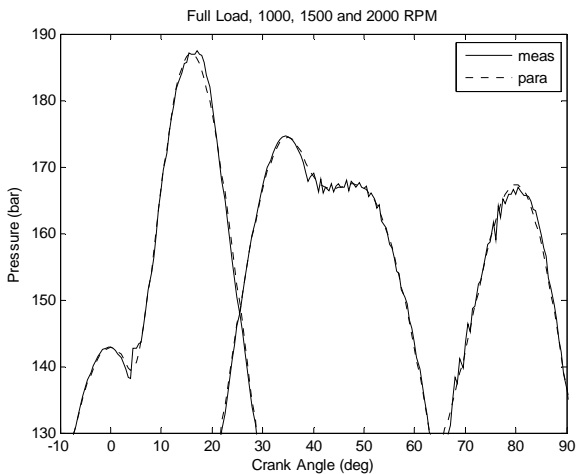


Figure 4. Zoom within the combustion region of Figure 3. From left to right traces at 1000 RPM, 1500 RPM and 2000 RPM respectively.

Figure 3 and Figure 4 depict some examples of the parameterizations obtained. Note that in order to improve visualization two of the traces have been shifted

in the crank angle domain 100 *degrees* each in Figure 3, and 35 *degrees* each in Figure 4.

As observed from Figure [3], the fit is systematically worse during intake and part of the compression than during combustion and expansion. This is to be anticipated due to the numerical weighting described in previous sections. The plots give an idea of the level of fit attainable with the current parameterization and of the complexities in conceiving a model capable of reproducing a wide range of combustion characteristics.

The corresponding examples for the partial load case are shown in Figures A1 and A2, in the appendix.

Once again it is pointed out that a formal validation of the results is not carried out here and we will be focusing on the reproduction of the frequency content of the original signal and the physical information reflected by some of the parameters

## FREQUENCY CONTENTS AND ATTENUATION

The Fast Fourier Transform (FFT) is used to compute the frequency contents of the measured and parameterized pressures, respectively. A Hanning window is applied to the measurements in order to correct for discrepancies in starting and ending levels of the pressure signals.

The sound pressure level (SPL) is in literature, see [3] and [4], defined as:

$$SPL = 20 \text{Log}_{10} \left( \frac{\tilde{p}}{p_0} \right)$$

where  $p_0$  is the standard reference level of  $2 \times 10^{-5} \text{ Pa}$  and  $\tilde{p}$  is denoted as the effective value of the pressure and defined as:

$$\tilde{p} = \sqrt{\frac{1}{T} \int_0^T p(t)^2 dt}$$

Figure 5 shows the SPL of the full load pressure trace included previously in Figure 1. It illustrates the effect of low pass filtering in the frequency domain, as will be performed herein in order to improve visualization.

Figure 6 includes the SPL curves at 800 RPM in full load and motored cases. The contribution of the motored trace (pure and adiabatic compression) is only representative in the low frequency range, this highlights the importance of the combustion model selected, and consequently the high correlation between noise and the heat release rate, in agreement with [1].

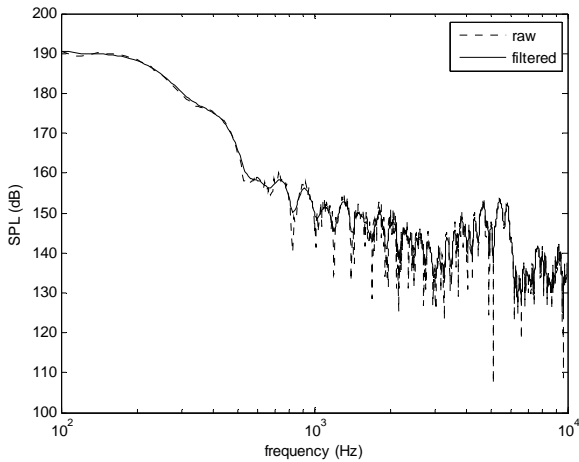


Figure 5. SPL for pressure trace at full load and 800 RPM

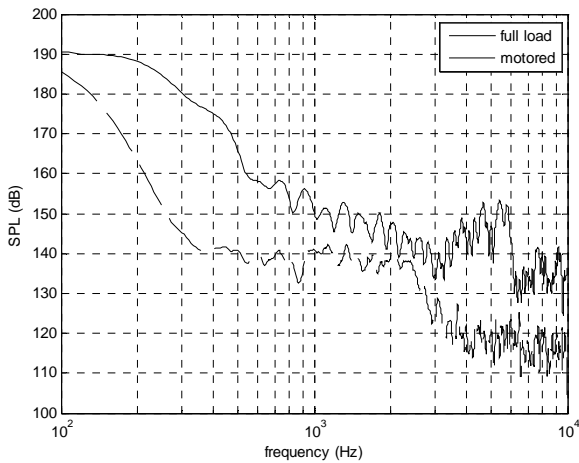


Figure 6. Filtered SPL for pressure traces for full load and motored, at 800 RPM.

## STRUCTURAL ATTENUATION

Previous work presented in [1] and [5] confirmed the similarities between noise attenuating properties of engine structures from different manufacturers. Hence the standard "SA1-7dB" attenuation curve, see [3] and Figure 7, is picked for filtering of the pressure traces to yield a prediction for radiated engine noise. This result will in turn be filtered for human perception using the A-weighting to give an output in dB(A). Note that all SPL calculations performed henceforth will include these two filters.

It is important to highlight that the procedure employed here for calculating the SPL assumes free field conditions

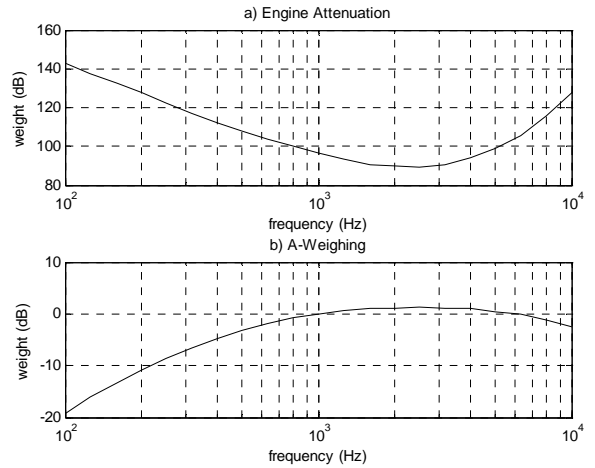


Figure 7. a) Average engine structure attenuation. SA1-7dB or Lucas filter. b) A- weighing for human perception

## RESULTING SOUND PRESSURE

Using the procedure described above Figure 8 and Figure 9 are generated, they show predicted SPL curves for the foregoing examples.

It is readily noticeable that the parameterizations work well in the low frequency range, namely up to 500 Hz. Between 500-1000 Hz a zone of uncertainty appears where the model fluctuates around the measurement generated trace with differences ranging the 5 dB, thereafter the model based output yields much lower levels. The modeled curves surpassed the "measured" ones at certain frequencies and this is probably due to the lack of smoothness in the transitions of the model, for example between combustion and expansion, as described in previous sections.

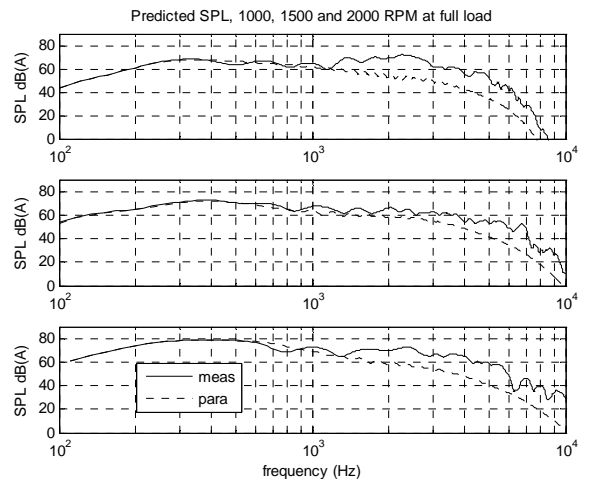


Figure 8. SPLs in full load at 1000 (upper), 1500 (middle) and 2000 (lower) RPM, respectively.

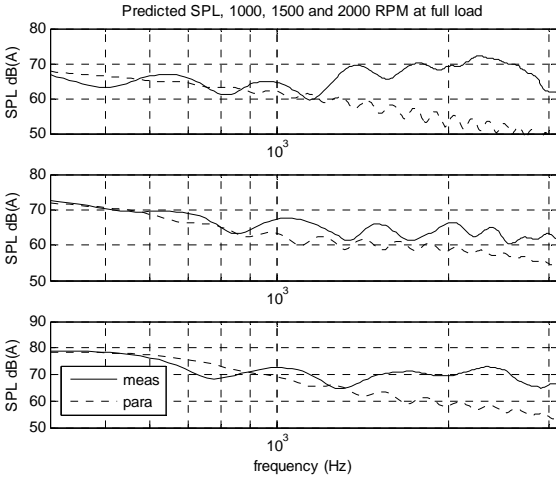


Figure 9. Zoom of previous plot, divergence range

The corresponding partial load plots are included in the appendix; see Figures A3 and A4 respectively. In these the parameterizations behave similarly to the ones just shown; although there appears to be a slightly better fit between the two traces and for each RPM.

The Lucas filter and the characteristic human perception or A-weighting, both indicate that the frequency range between 500 Hz and 5 kHz is of great importance, see [3]. We will therefore also propose a method to improve the model in this range.

Figures A7 and A10 in the appendix show plots of the difference between parameterized and measured SPL curves, for full load and partial load cases, and the whole selection of speeds. Unfortunately there seems to be no visible patterns.

#### COMPENSATION FOR HIGHER FREQUENCIES

The large deviation between model output and measurement obtained curves, in the frequency range over 1000 Hz, reflects the fact that the model employed here does not account for several other higher frequency phenomena that take place in the combustion chamber. In [10] the importance of resonances due to the oscillations of burned gases in the combustion chamber is pointed out as one of the main excitation sources of the engine block during the combustion process.

The ultimate goal of the parameterizations is to give reasonably accurate predictions up to the order of 5 kHz. In order to improve correlation between measurements and model predictions in this higher frequency range a pragmatic approach is taken. The well known “*sine cardinal*” function might in this context be given the physical interpretation of a pulsating pressure with broad bandwidth frequency content. Hence, it could be a way of introducing combustion chamber resonances for instance.

#### The *sinc* function

$$f(t) = \text{sinc}(\omega t)$$

as it is perhaps better known, becomes a step function in the frequency domain upon applying the Fourier transform, and vice versa; see, e.g. [6] and [7]. Figure 10 illustrates this fact for  $\omega=1$  and  $\omega=2$ :

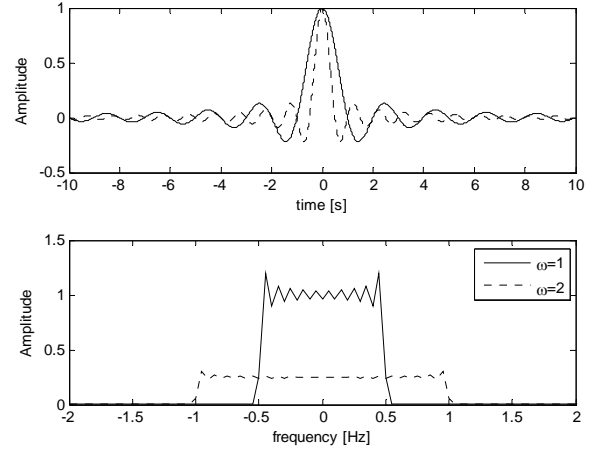


Figure 10. The *sinc* function and its Fourier transform. A short pulse in the time domain results in a broad bandwidth in the frequency domain, and vice versa.

The resulting Fourier transforms should in theory become perfect steps in the frequency domain; however the figure shows the effect of the numerical computation of the transform using a finite number of samples, the well known Gibbs phenomenon. This type of oscillations will be obtained in the SPL curves due to the numerical computation and due to lack of smoothness in the case of the parameterized pressure traces, and noise in the “measured” ones.

Now, by simply adding a new parameterized term governed by the *sinc* function and centered at for instance *start of combustion* a sort of amplitude compensation will result in the frequency domain, and in a specific frequency range. The augmented model becomes:

$$p'(\theta) = p(\theta) + p_{hf}(\theta)$$

Where the new component of the parameterization, namely  $p_{hf}$ , is built as follows:

$$p_{hf}(\theta) = \frac{\mu \sin[\gamma(\theta - \theta_{soc})]}{\theta - \theta_{soc}}$$

Where  $\mu$  and  $\gamma$  are new free parameters to be tuned and  $\theta_{soc}$  is the angle for the start of combustion. Note that the latter parameter has already been calculated for the non compensated model. This time it becomes

cumbersome to implement a procedure for finding optimal values of  $\mu$  and  $\gamma$ . Iteration and a qualitative comparison of the resulting *SPL* obtained from different sets of values yield for the full load case, the numbers included in Table 1.

RPM	$\mu$	$\gamma$	$\theta_{soc}$
1000	2.5	0.9	3.38
1500	1.5	0.9	2.77
2000	2	0.9	-4.5

Table 1. Parameters of the sinc compensation, full load.

Figure 11 and Figure 12 depict the corresponding predicted *SPL* curves.

As observed for these particular cases the fit to the measurements has been increased at higher frequencies; up to 2.8 kHz for 1000 RPM, up to 4 kHz for 1500 RPM and up to 5.5 kHz for 2000 RPM, respectively. These results indicate that the angular speed determines the action range of the *sinc* compensation. Notice that the  $\gamma$  selected has been the same at each RPM

The corresponding values for the partial load case are included in the appendix, see Table A1 and Figures A11 and A12. The parameterizations give slightly better fit in this case, which could be observed already in Figures A3 and A4, leaving a smaller margin of action for the *sinc* compensation. The fit is improved for the 2000 RPM plot up to 2.3 kHz in this case, no real improvement is observed for the other two angular speeds.

Apart of the likely similarity with resonance phenomena in the combustion chamber, we have no direct or unique physical interpretation of these two new parameters. The implementation of this *sinc* compensation is still under refinement and no further analysis is shown here.

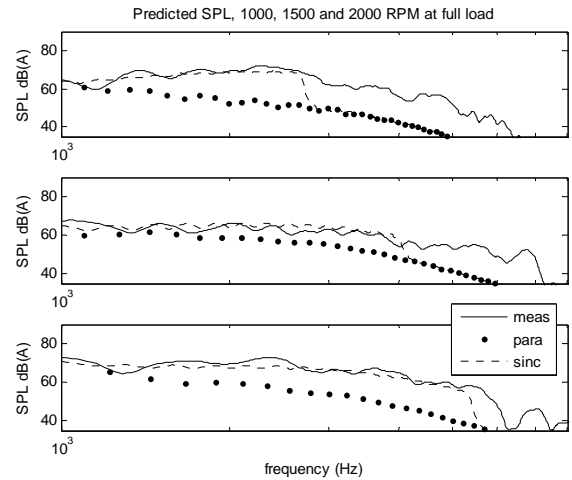


Figure 12. Zoom of Figure 11

## STATISTICAL CONSIDERATIONS

The cylinder pressure measurements were acquired with 50 cycles as mentioned before; Figure 13 shows the dispersion in the pressure traces with respect to the average for one specific case. As with other magnitudes in previous sections, a smoothing filter has been applied to the variance to improve visualization. Figures A17 and A18 in the appendix illustrate the scattering in the frequency domain; they depict the *SPL* curve for this case adding the standard deviation.

As noticed the dispersion appears during valve operation and combustion processes; but more markedly in the latter. This result brings forth the hypothesis of including a stochastic component directly linked to the combustion phenomena into any attempt of modeling. Figure 14 shows the corresponding dispersion at 4 different speeds in the full load case.

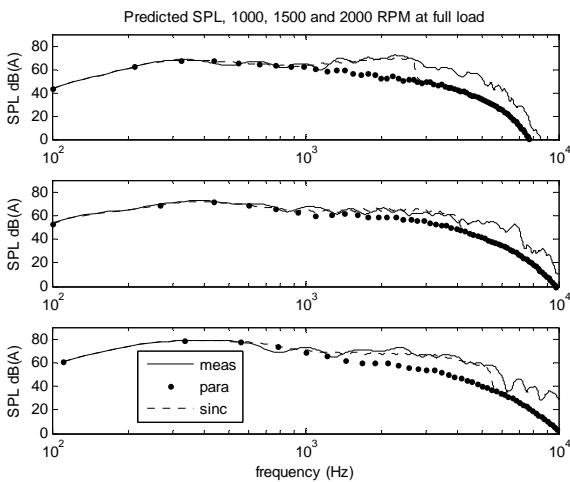


Figure 11. *SPL* for sinc compensated parameterization, 1000 (upper), 1500 (middle) and 2000 (lower) RPM at full load

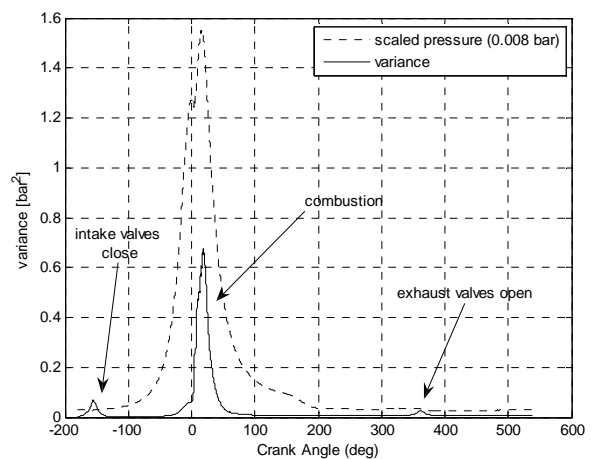


Figure 13. Pressure trace's variance in 50 cycles, full load and 1100 RPM

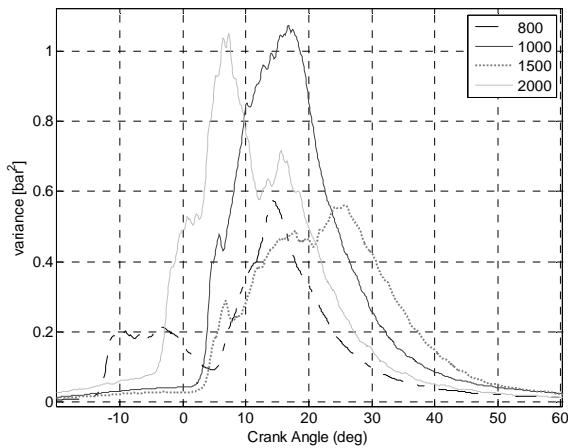


Figure 14. Pressure trace's variance in 50 cycles, combustion area, at full load, in the speed range: 800, 1000, 1500 and 2000 RPM

Plots including the variance of both full load and partial load, for each speed, are included in the appendix. In general terms the partial load case reveals a higher dispersion. With the observed trend, see Figure 14, a possible approach could be to model injection and combustion as two separate stochastic processes. The first would exhibit an approximately uniform distribution and the second a normal one, which could be centered on the angle for peak pressure. This analysis will be addressed in future work.

## CONCLUSIONS

Cylinder pressure traces have been parameterized in straightforward fashion with the advantage of rapid implementation and physical implications. Sound pressure levels were computed according to the average engine structure attenuation referred to as Lucas filter and the A-weighting. High correlation between predictions and measurements was encountered in the low frequency range (up to 500 Hz). A compensation term has been proposed based on the implementation of the *sine cardinal* function, emulating combustion resonance phenomena. By adding this term the model fit increased at higher frequencies. Our results indicate that the approach is interesting but desirable improvements are to decrease the number of parameters, ideally a direct equivalence among test and model parameters and to make possible a complete validation.

No treatment or analyses of phase have been included in this work; the focus has been centered on amplitudes at a first and early stage.

A short statistical description has also been presented which could lay a foundation for the inclusion of stochastic dependencies into future modeling and characterization of cylinder pressure.

## ACKNOWLEDGMENTS

Valuable contributions of Saban Eren and Per Gunnar Walter for the carrying out of measurements at SCANIA's test cells are acknowledged.

## REFERENCES

- [1] M. F. Russell and R. Haworth. Combustion Noise from High Speed Direct Injection Diesel Engines. SAE Paper 850973.
- [2] L. Eriksson, I. Andersson. *An Analytic Model for Cylinder Pressure in a Four Stroke SI Engine*. SAE Technical Paper no. 2002-01-0371.
- [3] D. Anderton, *Engine Noise & Vibration Control. Course Notes*. 1990 ed. The Institute of Sound and Vibration Research, Southampton University, 1990.
- [4] H. Bodén, U. Carlsson, R. Glav, H. P. Wallin och M. Åbom. *Ljud och Vibrationer*. 2001. ISBN 91-7170-434-5.
- [5] M.F. Russel and E. J. Cavanagh. *Establishing a target for control of diesel combustion noise*. SAE paper 790271 in Detroit SAE book p 80. "Diesel Engine Noise Conference" March 1979.
- [6] F. Gustafsson, L. Ljung, M. Millnert. *Signalbehandling*. Andra upplagan. ISBN 91-44-01709-X
- [7] P. Händel, R. Ottoson och H. Hjalmarsson. *Signalteori*. 3: upplagan 2002. ISBN 91-974087-2-7.
- [8] Weisstein, Eric W. *Nonlinear Least Squares Fitting*. From Math World. <http://mathworld.wolfram.com>
- [9] Ljung L., *System Identification, Theory for the User*. Second Edition 1999. ISBN 0-13-656695-2
- [10] A. Torregosa, A. Broatch, V. Marant and Y. Beauge. *Analysis of Combustion Resonance in DI Automotive Diesel Engines*. THIESEL 2002. Conference on Thermo- and Fluid Dynamics Processes in Diesel Engines

## CONTACT

MSc José Scarpatti  
 Engine Dynamics and Acoustics  
 Scania AB  
 phone: +46 8 553 52264  
 e-mail: jose.scarpatti@scania.com; scarpatti@ee.kth.se

## DEFINITIONS, ACRONYMS, ABBREVIATIONS

**RPM:** crank shaft angular speed

**CAD,  $\theta$ :** Crank angle in degrees

$\vec{\alpha}$  : parameter vector

$d\vec{\alpha}$  : offset parameter vector

$j$ : index for parameters

$n$ : total number of parameters

$\vec{p}$  : vector of sampled pressures

$i$ : index for samples

$m$ : total number of samples

$A$ : Jacobian matrix for parameters

$Q_N$ : weight matrix

$kc$ : polytropic exponent compression

$ke$ : polytropic exponent expansion

$V$  : volume

$P_0$ : intake pressure

$P_{soc}$ : pressure at start of combustion

$P_{eoc}$ : pressure at end of combustion

$P_{ex-ref}$ : Exhaust reference pressure

soc: start of combustion

eoc: end of combustion

$a_{vibe}, x_{vibe}$ : parameters in Vibe's correlation

$a_{exh}, y_{exh}$ : parameters in exhaust's correlation

$ivo$ : intake valve open.

$evo$ : exhaust valve open

$p_{hf}$ : high frequency pressure compensation

$sinc$ : sine cardinal function

$\mu, \gamma$  :  $sinc$  parameters

$\rho$ : fit index

## APPENDIX

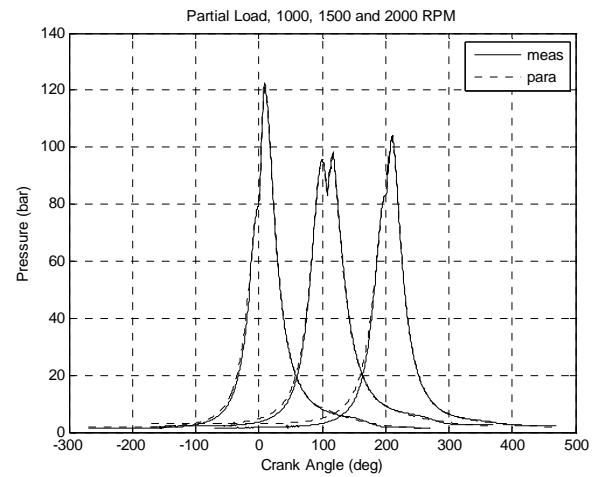


Figure A1. Measured and estimated partial load pressure traces at 1000 RPM, 1500 RPM and 2000 RPM respectively.

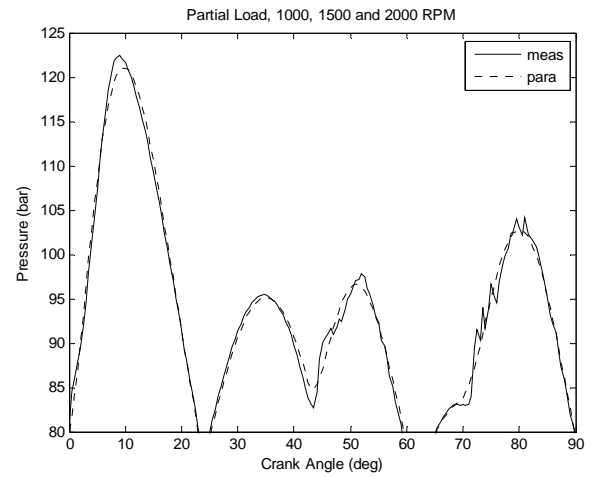


Figure A2. Zoom within the combustion region of Figure A1.

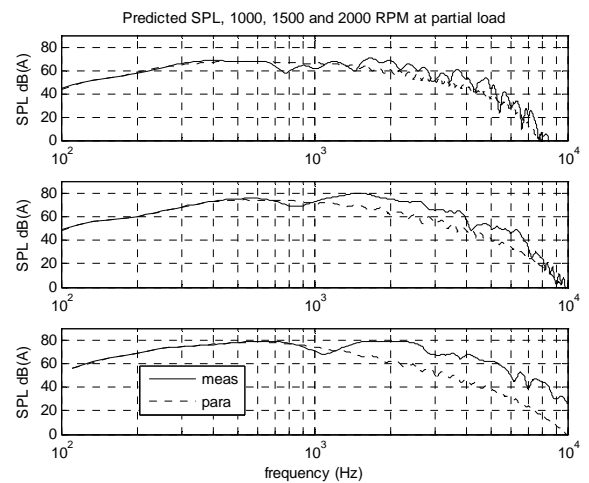


Figure A3. SPL in partial load at 1000, 1500 and 2000 RPM, respectively

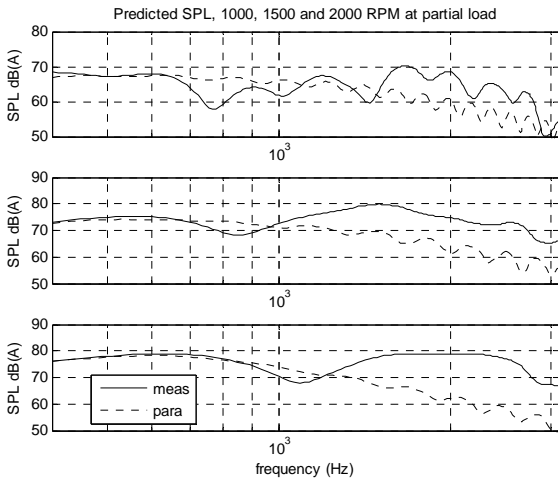


Figure A4. Zoom of figure A3

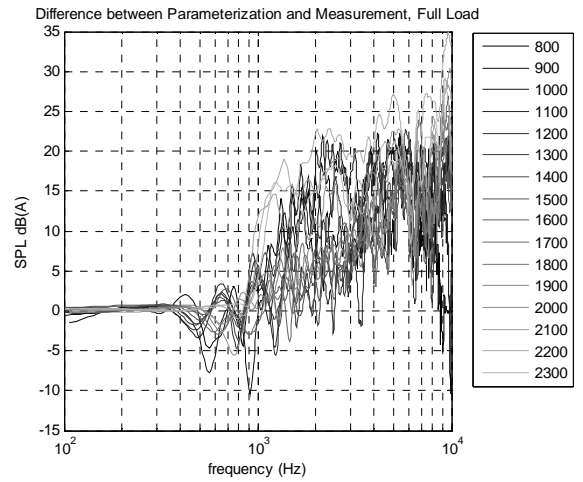


Figure A7. Difference in SPL from parameterized and measured p traces at full load

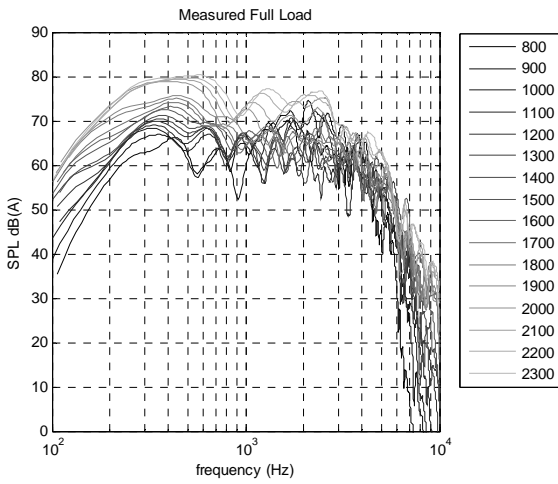


Figure A5. SPL from measured p traces at full load

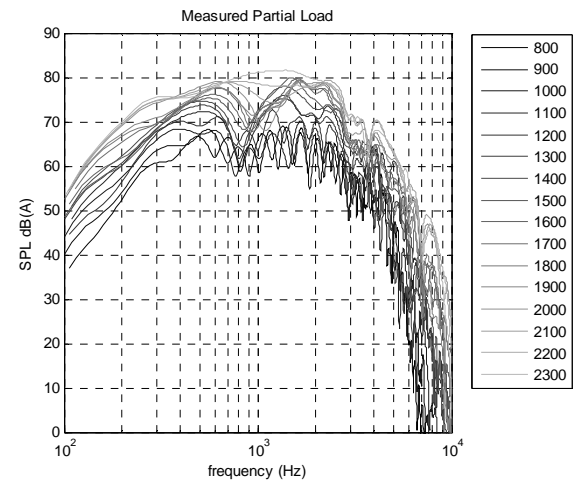


Figure A8. SPL from measured p traces at partial load

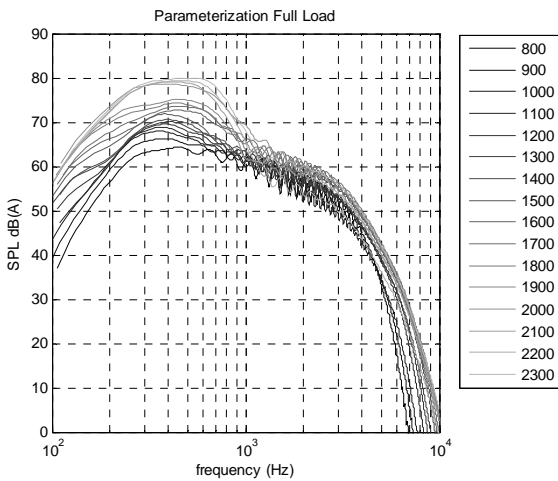


Figure A6. SPL from parameterized p traces at full load

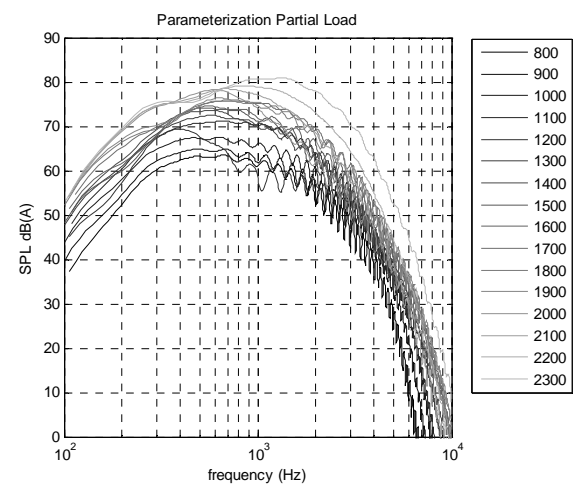


Figure A9. SPL from parameterized p traces at partial load

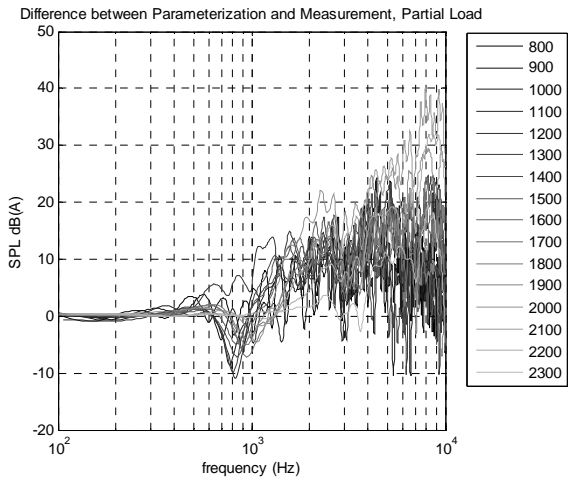


Figure A10. Difference in SPL from parameterized and measured p traces at partial load

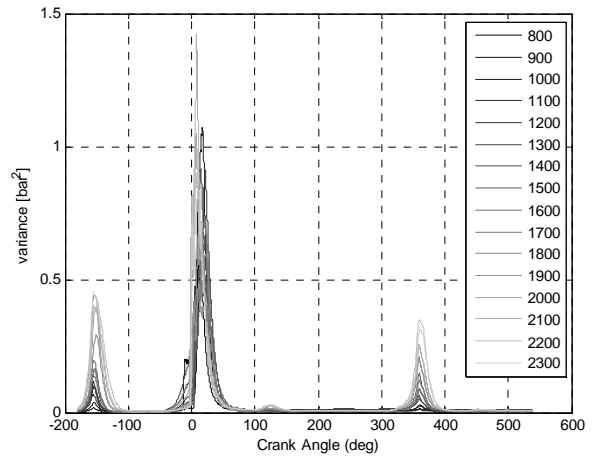


Figure A13. Variances full load

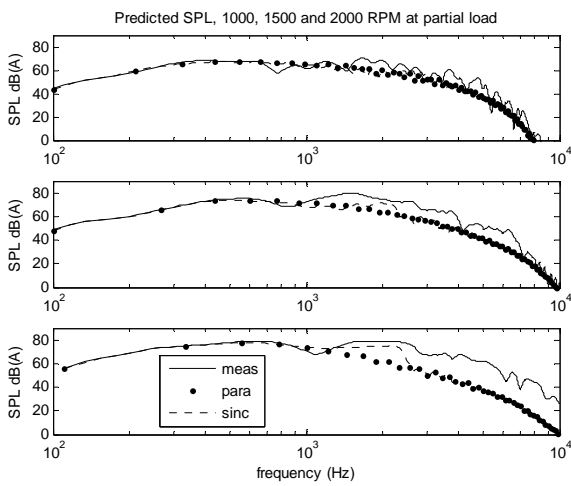


Figure A11. SPL for sinc compensated parameterization, 1000 (upper), 1500 (middle) and 2000 (lower) RPM at partial load

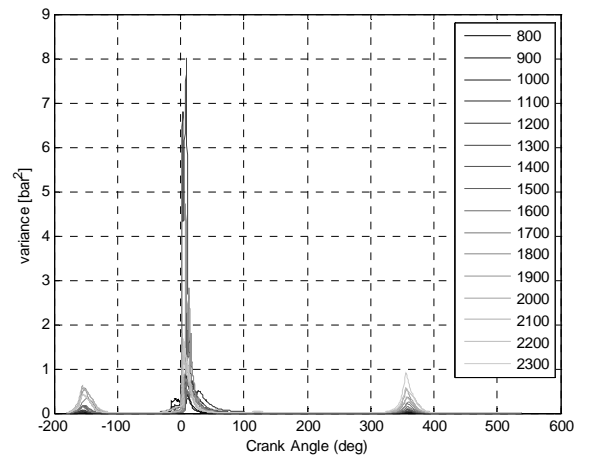


Figure A14. Variances partial load

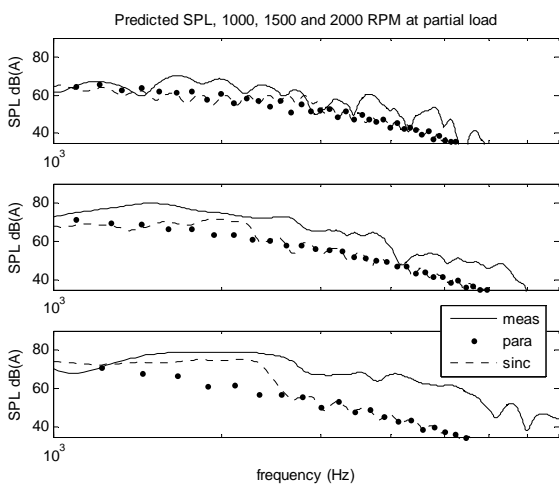


Figure A12. Zoom of figure A11

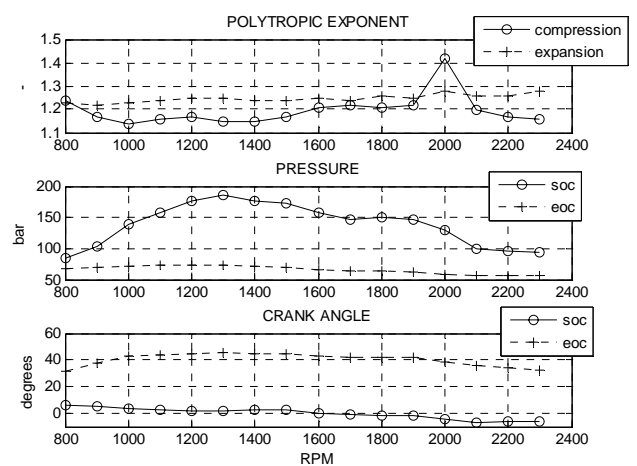


Figure A15. Tuned parameters full load

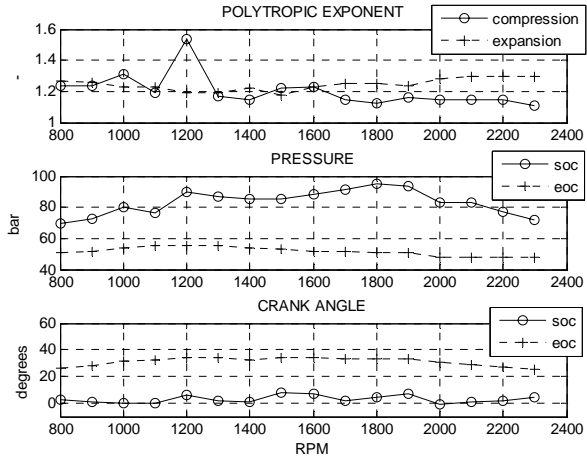


Figure A16. Tuned parameters partial load

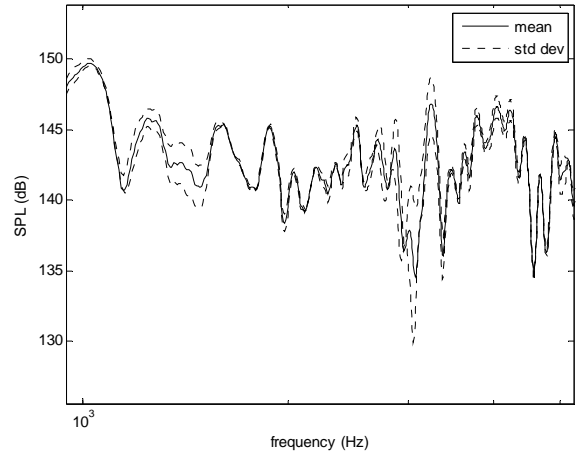


Figure A18. Zoom of figure A17.

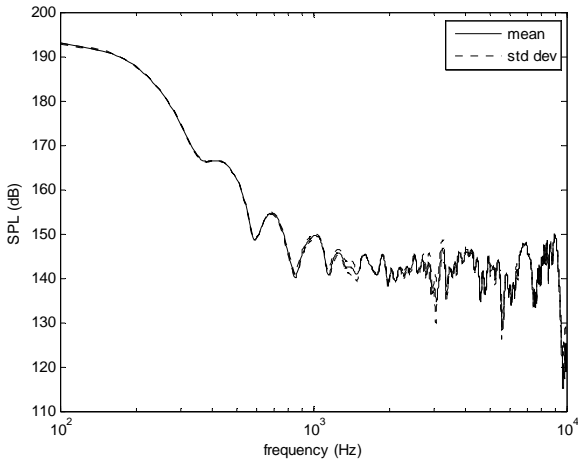


Figure A17. SPL for measured  $p$  trace including standard deviations, at 1100 RPM and full load.

RPM	$\mu$	$\gamma$	$\theta_{soc}$
1000	1	1	0.11
1500	2.2	0.5	7.69
2000	2.3	0.4	-0.77

Table A1 Parameters of the sinc compensation, partial load

RPM	kc [-]	ke [-]	Pex [bar]	Psoc [bar]	Peoc [bar]	soc [°]	eoc [°]	a_vibe [-]	x_vibe [-]	b_ex [-]	y_ex [-]	evo [°],	$\rho_{total}$	$\rho_{comb}$
800	1,24	1,27	0,97	69,47	50,64	2,46	26,28	8,22	1,50	0,12	1,17	96,50	87,15	99,99
900	1,24	1,26	0,85	72,29	51,80	1,35	27,89	7,45	1,52	0,12	1,13	94,00	87,77	99,99
1000	1,31	1,23	0,76	79,96	54,03	-0,11	31,45	7,09	1,49	0,11	1,12	93,00	97,13	99,99
1100	1,19	1,23	0,39	76,46	55,38	-0,37	32,33	5,61	1,32	0,15	0,94	85,50	89,2	99,99
1200	1,54	1,19	0,02	90,11	55,40	6,42	34,50	8,58	2,21	0,20	0,80	79,97	94,24	99,99
1300	1,17	1,19	-0,68	86,82	55,39	1,63	34,33	5,54	1,47	0,23	0,72	73,00	86,83	99,99
1400	1,15	1,22	-0,50	85,41	53,98	0,92	32,85	6,75	1,63	0,24	0,70	72,60	82,89	99,99
1500	1,22	1,18	-0,44	85,15	53,36	7,69	34,50	5,56	1,59	0,29	0,65	70,81	94,38	99,99
1600	1,23	1,23	-0,36	88,25	51,48	7,24	34,00	4,68	1,54	0,28	0,65	70,88	95,45	99,98
1700	1,15	1,25	0,76	91,74	51,66	1,95	33,34	3,41	1,27	0,29	0,70	70,96	81,4	99,99
1800	1,12	1,25	0,86	95,20	50,71	4,04	33,50	3,42	1,34	0,29	0,69	71,96	72,04	99,99
1900	1,16	1,24	0,89	93,44	50,64	6,66	33,50	3,39	1,40	0,30	0,68	71,96	81,35	99,99
2000	1,15	1,28	0,86	83,22	47,71	-0,77	30,77	6,64	1,88	0,27	0,71	76,95	76,53	99,99
2100	1,15	1,30	1,93	83,39	47,74	0,74	29,11	4,42	1,49	0,30	0,81	77,80	74,62	99,99
2200	1,15	1,30	1,88	77,31	48,05	2,24	27,55	2,88	1,17	0,31	0,82	77,09	71,51	99,99
2300	1,11	1,30	1,95	71,92	47,75	4,17	25,72	1,92	0,80	0,33	0,85	75,50	59,11	99,99

Table A2. Resulting parameters in partial load

RPM	kc [-]	ke [-]	Pex [bar]	Psoc [bar]	Peoc [bar]	soc [°]	eoc [°]	a_vibe [-]	x_vibe [-]	b_ex [-]	y_ex [-]	evo [°],	$\rho_{total}$	$\rho_{comb}$
800	1,24	1,23	1,59	84,51	67,99	6,55	32,00	7,70	1,74	0,08	1,90	135,62	91,03	99,99
900	1,17	1,22	2,32	103,82	69,99	5,00	37,39	8,46	1,84	0,05	2,08	132,50	86,26	99,99
1000	1,14	1,23	3,14	139,86	72,29	3,38	42,82	8,68	1,91	0,04	2,13	131,00	80,24	100
1100	1,16	1,24	3,98	157,36	73,04	2,57	43,94	7,79	1,97	0,04	2,10	130,50	86,06	100
1200	1,17	1,25	4,58	175,69	73,92	1,92	44,94	6,74	1,97	0,04	2,16	129,50	85,98	100
1300	1,15	1,25	5,10	186,15	73,96	1,80	45,40	5,99	1,99	0,04	2,15	128,50	83,16	100
1400	1,15	1,24	4,40	176,27	72,16	2,90	45,00	5,26	2,03	0,04	1,99	127,17	83,86	100
1500	1,17	1,24	4,57	171,96	69,88	2,77	44,47	5,33	2,14	0,04	1,97	126,00	87,8	100
1600	1,21	1,25	3,74	158,51	66,48	0,45	42,97	5,38	2,01	0,04	1,86	124,00	92,91	100
1700	1,22	1,24	3,49	145,70	63,93	-0,80	42,00	5,70	2,08	0,04	1,80	121,50	94,02	100
1800	1,21	1,26	3,92	149,62	63,19	-1,52	42,00	5,88	2,24	0,05	1,76	120,00	91,82	100
1900	1,22	1,25	4,19	146,08	62,04	-1,61	41,92	5,76	2,25	0,05	1,68	118,00	92,49	100
2000	1,42	1,28	3,31	129,31	59,30	-4,50	38,84	7,76	2,21	0,07	1,44	111,00	98,92	99,99
2100	1,20	1,26	2,58	99,15	57,45	-7,35	35,82	8,53	2,74	0,11	1,16	103,00	88,47	99,99
2200	1,17	1,26	2,41	95,39	56,61	-6,33	34,20	7,43	2,65	0,13	1,10	102,00	81,16	99,99
2300	1,16	1,28	2,40	94,09	56,15	-5,82	32,85	7,40	2,83	0,16	1,00	100,50	74,67	99,99

Table A3. Resulting parameters in full load

Fit Index:

$$\rho = \frac{1}{m} \sum_{i=1}^m \left( 1 - \frac{(p_i - p_{par,i})^2}{p_i^2} \right), \text{ where } p_i \text{ stands for observed pressure, } p_{par,i} \text{ for parameterized value and } m \text{ for the number of samples.}$$